

# Preparation and Mössbauer spectroscopic studies of 1',1'''-diacetyl- and 1'-acetyl-1'''-(1-naphthylimino-ethyl)biferrocenes and their partially oxidized biferrocenium salts

Ho-Hsiang Wei and Ing-Shiou Hwang

Department of Chemistry, Tamkang University, Tamsui (Taiwan)

Ming-Chu Cheng and Yu Wang

Department of Chemistry, National Taiwan University, Taipei (Taiwan)

(Received July 22, 1993; in revised form September 22, 1993)

## Abstract

The 1',1'''-diacetyl and 1'-acetyl-1'''-(1-naphthylimino-ethyl)substituted biferrocenes,  $\text{CH}_3\text{CO}-\text{Fc}-\text{Fc}-\text{COCH}_3$  (**1**) and  $\text{CH}_3\text{CO}-\text{Fc}-\text{Fc}-\text{C}(\text{CH}_3)=\text{N}-\text{np}$  (**2**), where  $\text{Fc} = \text{C}_5\text{H}_4\text{FeC}_5\text{H}_4$  and  $\text{np} = 1\text{-naphthyl}$ , and the corresponding monocations as salts with  $\text{I}_3^-$ ,  $\text{I}_5^-$ ,  $\text{FeCl}_4^-$  and  $\text{CuI}_2^-$  have been prepared. The crystal structures of **1** and **2** have been determined. The temperature-dependent Mössbauer spectra of the biferrocenium salts with the exception of the  $\text{I}_3^-$  salt from **2** revealed them all to be of the mixed-valence type. The interaction between counter anions and the biferrocenium cations is discussed.

**Key words:** Ferrocene; Acetyl; Mössbauer spectroscopy

## 1. Introduction

The study of electron transfer in mixed-valence metallic complexes provides insight into electron transfer in biological processes, and many model systems have been developed [1]. It has been found from  $^{57}\text{Fe}$ -Mössbauer spectroscopic studies that the valence state of the iron atoms in 1',1'''-dialkyl- [2–6] and halogen-substituted [7] biferrocenium salts of  $\text{I}_3^-$ ,  $\text{FeCl}_4^-$ ,  $\text{ZnCl}_4^-$ ,  $\text{PF}_6^-$ ,  $\text{SnCl}_6^{2-}$  and picrate, can be classified in the solid state in terms of the extent of delocalization or the degree of interaction between ferrocene (Fc) and ferrocenium ( $\text{Fc}^+$ ) moieties [8]. One category is a mixed-valence type, which has two independent valence states of iron atoms corresponding to  $\text{Fe}^{\text{II}}$  and  $\text{Fe}^{\text{III}}$ . The other is an average valence type, which has only one equivalent non-integral valence state of iron atom on the Mössbauer time scale [8].

The present studies were aimed at clarifying the effect of acetyl and naphthylimine substituents and that of the counteranion, of  $\text{I}_3^-$ ,  $\text{CuI}_2^-$  and  $\text{FeCl}_4^-$ , on the valence state of iron atoms in the biferrocenium derivatives. Thus 1',1'''-diacetyl-biferrocene, 1'-acetyl-1'''-(1-naphthylimino-ethyl)biferrocene and a series of their salts with  $\text{I}_3^-$ ,  $\text{I}_5^-$ ,  $\text{CuI}_2^-$  and  $\text{FeCl}_4^-$  were prepared. The structures and electronic valence states of these compounds were studied by means of X-ray diffraction, cyclovoltammetry, and IR and Mössbauer spectroscopy.

## 2. Experimental details

### 2.1. Preparation of compounds

1',1'''-Diacetyl-biferrocene ( $\text{CH}_3\text{CO}-\text{Fc}-\text{Fc}-\text{COCH}_3$ ) (**1**) was prepared by the published method [9] and its identity confirmed by IR, NMR, and mass spectroscopy. The single crystal used for crystallography was grown in  $\text{CH}_2\text{Cl}_2/\text{benzene}$  (1 : 1). M.p.  $192^\circ\text{C}$  Anal. Found: C, 63.19; H, 4.88  $\text{C}_{24}\text{H}_{22}\text{O}_2\text{Fe}_2$ , calcd.: C, 63.48; H, 4.88%.

Correspondence to: Professor H.-H. Wei.

1'-Acetyl-1'''-(1-naphthylimino-ethyl)biferrocene ( $\text{CH}_3\text{CO}-\text{Fc}-\text{Fc}-\text{C}(\text{CH}_3)=\text{N}-\text{np}$ ) (**2**) was first prepared in the present study by Schiff-base condensation between diacetyl-biferrocene with 1-amino-naphthalene [10]. A solution of **1** (0.01 mol) and 1-amino naphthalene (0.02 mol) in toluene (200 ml) was added to a suspension of  $\text{Al}_2\text{O}_3$  (0.90 g) in toluene (100 ml). The mixture was refluxed for five days under  $\text{N}_2$ . The reaction products were separated by column chromatography on silica gel. The compound **2** (0.4 g) was eluted by  $\text{CH}_2\text{Cl}_2$  and a mixture of  $\text{CH}_2\text{Cl}_2$ /benzene (1:1), and a small portion (0.01 g) of 1',1'''-bis(1-naphthylimino-ethyl)biferrocene ( $\text{np}-\text{N}=\text{C}(\text{CH}_3)\text{C}-\text{Fc}-\text{Fc}-\text{C}(\text{CH}_3)=\text{N}-\text{np}$ ) was also eluted. The single crystal of **2** for crystallography was grown in  $\text{CH}_2\text{Cl}_2$ /benzene (1:1). M.p.  $178^\circ\text{C}$ . Anal. Found: C, 70.21; H, 5.05; N, 2.41.  $\text{C}_{34}\text{H}_{29}\text{NOFe}_2$  calcd.: C, 70.50; H, 5.01 N, 2.42%.

Mixed-valence **1** and **2** salts with  $\text{I}_5^-$  (**1a**) and  $\text{I}_3^-$  (**2a**) anions were prepared by the simple procedure previously described for the  $\text{I}_3^-$  salt of biferrocenium [10]. The mixed-valence **1** and **2** salts with  $\text{FeCl}_4^-$  (**1b** and **2b**) and  $\text{CuI}_2^-$  (**5**) were prepared by the procedure previously used for the  $\text{FeCl}_4^-$  and  $\text{CuI}_2^-$  salts of biferrocenium [3,10]. Anal. Found: C, 26.61; H, 2.23.  $\text{C}_{24}\text{H}_{22}\text{Fe}_2\text{I}_5$  (**1a**) calcd.: C, 26.47; H, 2.02%. Found: C, 43.05; H, 3.23; N, 1.50.  $\text{C}_{34}\text{H}_{29}\text{NOFe}_2\text{I}_3$  (**2a**) calcd.: C, 42.53; H, 3.02; N, 1.46%. Found: C, 52.51; H, 3.61; N, 1.79.  $\text{C}_{34}\text{H}_{29}\text{NOFe}_3\text{Cl}_4$  (**2b**) calcd.: C, 52.53; H, 3.74; N, 1.80%.

## 2.2. Physical measurements

The crystal data were obtained on a CAD-4 diffractometer with graphite-monochromated Mo  $\text{K}\alpha$  radiation. Total number of reflections for **1**, 1766 ( $1441 > 2.0\sigma(I)$ ) and for **2**, 4790 ( $3209 > 1.8\sigma(I)$ ) were measured up to  $2\theta$  of  $50^\circ$  in the  $+h$ ,  $+k$ ,  $+l$  octants. The structure was solved by the heavy atom method and subsequent difference Fourier maps followed by full-matrix least-squares refinement; the final agreement indices are  $R(F) = 0.026$ ,  $R_w(F) = 0.026$  for **1** and  $R(F) = 0.041$ ,  $R_w(F) = 0.028$  for **2** respectively. A film method X-ray crystal structural analysis for the compound **1** was reported some time ago by Kaluski and

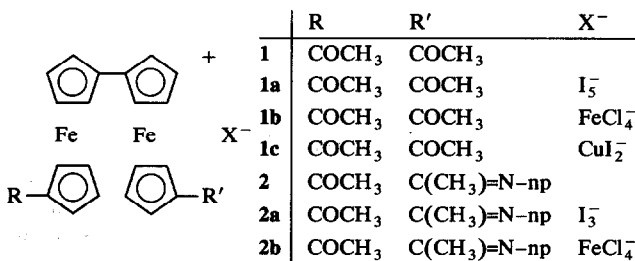


Fig. 1. 1',1'''-Substituted biferrocenes and biferrocenium salts.

TABLE 1. Crystallographic data for  $\text{COCH}_3-\text{Fc}-\text{Fc}-\text{COCH}_3$  (**1**) and  $\text{COCH}_3-\text{Fc}-\text{Fc}-\text{C}(\text{CH}_3)=\text{N}-\text{np}$  (**2**)

	1	2
Formula	$\text{Fe}_2\text{C}_{24}\text{O}_2\text{H}_{22}$	$\text{Fe}_2\text{C}_{34}\text{ONH}_{29}$
Formula weight	454.13	579.30
Diffractometer	CAD4	CAD4
Space group	$P2_1/n$	$P\bar{1}$
$a$ , Å	8.589(3)	11.170(4)
$b$ , Å	18.978(6)	11.275(4)
$c$ , Å	5.811(4)	11.454(8)
$\alpha$ , °	90	113.89(5)
$\beta$ , °	104.50(6)	101.40(5)
$\gamma$ , °	90	79.23(3)
$V$ , Å <sup>3</sup>	917.0(8)	1283.7(11)
$Z$	2	2
$D(\text{calc})$ , $\text{g cm}^{-3}$	1.645	1.499
$\lambda(\text{Mo K}\alpha)$ , Å	0.71069	0.71069
$F(000)$	468	600
unit cell detn; #; $2\theta$ range	24, (18.46–41.76)	24, (19.52–27.34)
scan type	$\theta/2\theta$	$\theta/2\theta$
$2\theta$ scan width, deg	$2(0.8 + 0.35 \tan\theta)$	$2(1.0 + 0.35 \tan\theta)$
$2\theta$ range, deg	2–50	2–50
$\mu(\text{Mo K}\alpha)$ , $\text{cm}^{-1}$	16.0	11.6
Crystal size(mm)	$0.80 \times 0.80 \times 1.00$	$0.50 \times 0.60 \times 0.50$
Temperature (K)	298	298
No. of meas. reflns.	1766	4790
No. of unique reflns.	1604	4517
No. of obs. reflns ( $I > 2\sigma(I)$ )	1441	3209
No. of refined params	172	343
$R$ , $R_w^*$	0.026, 0.027	0.041, 0.028
Minimized function	$\sum w  F_o - F_c ^2$	$\sum_w  F_o - F_c ^2$
Weighting scheme	$1/\sigma^2(F_o)$	$1/\sigma^2(F_o)$
$g(\text{second.ext.coef.}) \times 10^4$	1.23	0
$(\Delta/\sigma)_{\text{max}}$	0.033	0.022
$(\Delta\rho)_{\text{max, min}} \text{e}\text{Å}^{-3}$	0.34, -0.3	0.40, -0.36
Computation program	NRCVAX **	NRCVAX **

\*  $R = [\sum |F_o - F_c| / F_o]$ ;  $R_w = [\sum w(|F_o - F_c|^2 / \sum w(|F_o|^2))]^{1/2}$ ;  $\sigma^2(F_o)$  from counting statistics. \*\* NRCVAX E.J. Gabe, Y. Le Page, J.-P. Charland, F.L. Lee, and P.S. White, *J. Appl. Cryst.*, 22 (1989) 384.

Gusev [11]. The crystallographic data for **1** and **2** are listed in Table 1. Infrared spectra were recorded on a Shimadzu IR-470 infrared spectrophotometer. Cyclic voltammograms of **1** and **2** were obtained with a CV-27 potentiostat combined with a standard three-electrode configuration. A platinum button was used as the working electrode and  $\text{Ag}/\text{AgClO}_4$  as reference electrode.  $^n\text{Bu}_4\text{NBF}_4$  (0.05 M) in  $\text{CH}_2\text{Cl}_2$  was used as supporting electrolyte. The half-wave potentials at room temperature were: for **1**  $E_{1/2}(1) = 0.72$ ,  $E_{1/2}(2) = 1.07$  V; for **2**  $E_{1/2}(1) = 0.66$ ,  $E_{1/2}(2) = 0.97$ ,  $E_{1/2}(3) = 1.16$  V.

The  $^{57}\text{Fe}$  Mössbauer spectra were obtained on an Austin S-600 Mössbauer spectrometer of constant acceleration;  $^{57}\text{Co}(\text{Pd})$  was used as the radiation source. Iron foil was used as the standard for the isomer shift.

### 3. Results and discussion

The results of the single-crystal X-ray studies of **1** and **2** are first discussed. The ORTEP stereoscopic views of the compounds **1** and **2** are shown in Figs. 2 and 3. Selected bond lengths and angles for **1** and **2** are listed in Tables 2 and 4, and atomic coordinates and equivalent isotropic displacement coefficients in Tables 3 and 5. The molecular structures of **1** and **2** show some interesting features. The space groups of the crystals **1** and **2** are  $P2_1/n$  and  $P\bar{1}$ , respectively.

Both **1** and **2** show a *trans* conformation with the two iron atoms on opposite sides of the planar fulvenide ligands. This *trans*-conformation of the ferrocenyl moieties is a requirement for the formation of the mixed-valence biferrocenium monocation [12]. As can be seen from Tables 2 and 4, the mean bond distances between the iron atom and the five carbon atoms of a given ring are 2.050(3) and 2.040(4) Å for the rings [C(1)–C(5)] and [C(6)–C(10)] of **1** respectively. The mean bond distance between the Fe1 and the five carbon atoms of ring(I) and ring(II) for **2** are 2.036(4) and 2.036(5) Å, respectively, these distances being shorter than that of 2.045 Å observed for ferrocene [13]. However, the mean bond distances between the Fe2 and the five carbon atoms of ring(III) and ring(IV) are 2.045(5) and 2.041(5) Å, respectively, which are close to that of 2.045 Å observed for ferrocene [12].

The centroid–centroid (c-c) distance between the rings [C(1)–C(5)] and [C(6)–C(10)] for **1** is 3.301(2) Å (estimated from Table 2). The c-c distance between

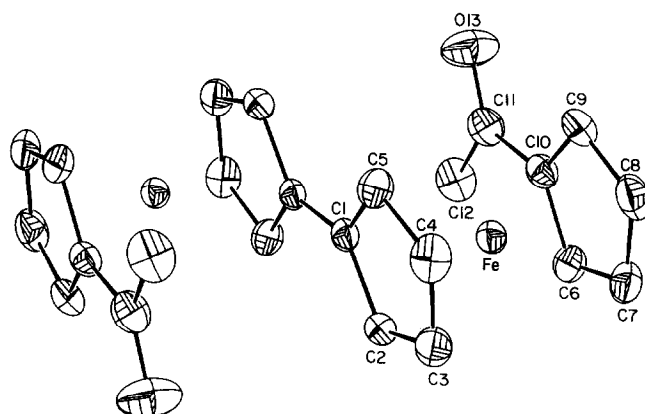


Fig. 2. ORTEP stereoview of  $\text{COCH}_3\text{-Fc-Fc-COCH}_3$  (**1**) with hydrogen atoms omitted (50% probability thermal ellipsoids).

ring(I) and ring(II) for **2** is 3.285(2) Å (estimated from Table 4), this is slightly shorter than that of 3.302(2) Å between ring(III) and ring(IV).

There are no significant deviations from regularity and planarity of the cyclopentadienide rings for **1** and **2**. The two rings in each ferrocenyl group of **1** and **2** are essentially eclipsed. The dihedral angles between rings [C(1)–C(5)] and [C(6)–C(10)] in **1** is 2.2° and that between rings (I) and (II) in **2** is 3.9°, and the stagger angle between rings (III) and (IV) is 32.5°.

The important IR absorption bands of C–H bending of cyclopentadienyl ring, CO stretching of acetyl and CN stretching of naphthylimine for the compounds are listed in Table 6. A previous report [14] on mixed-valence biferrocenium ion indicated that the C–H bend-

TABLE 2. Selected bond distances (Å) and angles (°) of  $\text{Fe}_2\text{C}_{24}\text{O}_2\text{H}_{22}$  for **1**

Distances					
Fe–C(1)	2.075(3)	C(1)–C(5)	1.422(4)	Fe–C(2)	2.050(3)
C(2)–C(3)	1.422(4)	Fe–C(3)	2.036(3)	C(3)–C(4)	1.409(5)
Fe–C(4)	2.041(3)	C(4)–C(5)	1.419(4)	Fe–C(5)	2.048(3)
C(6)–C(7)	1.408(4)	Fe–C(6)	2.029(3)	C(6)–C(10)	1.429(4)
Fe–C(7)	2.039(3)	C(7)–C(8)	1.417(5)	Fe–C(8)	2.049(3)
C(8)–C(9)	1.409(5)	Fe–C(9)	2.042(3)	C(9)–C(10)	1.427(4)
Fe–C(10)	2.041(3)	C(10)–C(11)	1.470(4)	C(1)–C(1) <sup>a</sup>	1.457(5)
C(11)–C(12)	1.493(5)	C(1)–C(2)	1.429(4)	C(11)–O(13)	1.218(4)
ring[C(1) ~ C(5)]–Fe	1.656(2)	ring[C(6) ~ C(10)]–Fe	1.645(2)		
Angles					
C(2)–Fe–C(6)	107.1(1)	C(3)–Fe–C(7)	104.9(1)	C(4)–Fe–C(8)	106.5(1)
C(5)–Fe–C(9)	109.6(1)	C(1) <sup>a</sup> –C(1)–C(2)	125.7(3)	C(1) <sup>a</sup> –C(1)–C(5)	126.6(3)
C(1)–Fe–C(10)	110.2(1)	C(2)–C(1)–C(5)	107.7(2)	C(1) <sup>a</sup> –C(1)–C(2)	125.7(3)
C(7)–C(8)–C(9)	108.2(3)	C(1) <sup>a</sup> –C(1)–C(5)	126.6(3)	C(8)–C(9)–C(10)	108.3(3)
C(2)–C(1)–C(5)	107.7(3)	C(6)–C(10)–C(9)	106.9(3)	C(1)–C(2)–C(3)	107.6(3)
C(6)–C(10)–C(11)	128.1(3)	C(2)–C(3)–C(4)	108.3(3)	C(9)–C(10)–C(11)	124.9(3)
C(3)–C(4)–C(5)	108.3(3)	C(10)–C(11)–C(12)	117.7(3)	C(1)–C(5)–C(4)	108.0(3)
C(10)–C(11)–O(13)	120.6(3)	C(7)–C(6)–C(10)	108.4(3)	C(12)–C(11)–O(13)	121.7(3)
C(6)–C(7)–C(8)	108.1(3)				

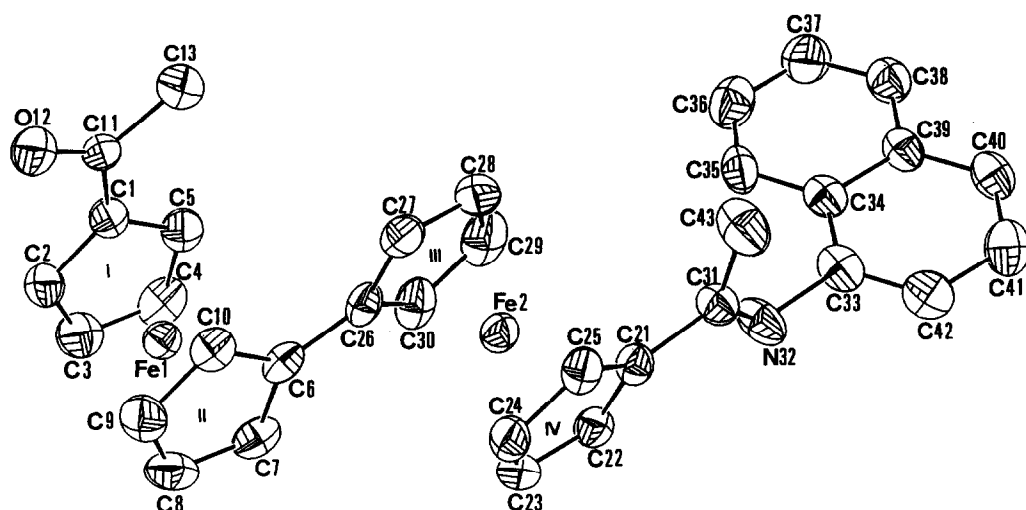
<sup>a</sup> indicates  $-x, 1-y, -z$ .

TABLE 3. Atomic parameters  $x$ ,  $y$ ,  $z$  and  $B_{\text{iso}}$ . e.s.d.'s refer to the last digit printed

	$x$	$y$	$z$	$B_{\text{eq}}$
Fe	0.01499(4)	0.635716(18)	0.00612(7)	1.713(18)
C1	0.0547(3)	0.52824(12)	0.0531(5)	1.74(11)
C2	0.0591(4)	0.56243(14)	0.2739(5)	2.12(13)
C3	0.1834(4)	0.61383(15)	0.3124(6)	2.55(13)
C4	0.2539(4)	0.61215(15)	0.1181(6)	2.70(14)
C5	0.1736(3)	0.56023(14)	-0.0444(6)	2.21(13)
C6	-0.1963(4)	0.68320(15)	0.0080(6)	2.44(13)
C7	-0.0708(4)	0.73295(15)	0.0595(6)	2.82(15)
C8	0.0005(4)	0.73513(15)	-0.1354(6)	2.92(14)
C9	-0.0803(4)	0.68649(15)	-0.3074(6)	2.48(13)
C10	-0.2044(3)	0.65382(13)	-0.2211(5)	2.01(11)
C11	-0.3129(3)	0.59853(15)	-0.3467(6)	2.56(13)
C12	-0.4321(4)	0.56836(21)	-0.2258(8)	3.33(17)
O13	-0.3078(3)	0.57978(12)	-0.5452(4)	4.37(12)

ing bands in IR spectra can be employed to tell whether a given mixed-valence biferrocene is delocalized or not. This band is seen at  $815\text{ cm}^{-1}$  for the ferrocene (Fe(II) moiety) and  $851\text{ cm}^{-1}$  for the ferrocenium (Fe(III) moiety) in biferrocenium triiodide [14].

1',1'''-Diacetylbiferrocene and 1'-acetyl-1'''-(1-naphthylimino-ethyl)biferrocene show strong C-H bending bands at  $814$  and  $829\text{ cm}^{-1}$  respectively. The oxidized compounds **1a**, **b**, **c** show two bands at  $820$ – $929$  and  $835$ – $854\text{ cm}^{-1}$ , and two bands at  $831$  and  $850\text{ cm}^{-1}$  for **2b**. These indicate that the intramolecular electron transfer is faster on the IR time scale. In addition, the fact that the C-H bending vibration for **2a** is the same as that for unoxidized **2** implies that the oxidation does not take place at the iron atoms in biferrocenyl moiety.

Fig. 3. ORTEP stereoview of  $\text{COCH}_3\text{-Fc-Fc-C(CH}_3\text{)=N-np}$  (**2**) with hydrogen atoms omitted (50% probability thermal ellipsoids).TABLE 4. Selected bond distances ( $\text{\AA}$ ) and angles ( $^\circ$ ) of  $\text{Fe}_2\text{C}_{34}\text{ONH}_{29}$  (**2**)

Distances					
Fe(1)–C(1)	2.025(4)	Fe(1)–C(2)	2.034(4)	Fe(1)–C(3)	2.050(4)
Fe(1)–C(4)	2.043(4)	Fe(1)–C(5)	2.029(4)	Fe(1)–C(6)	2.039(4)
Fe(1)–C(7)	2.034(4)	Fe(1)–C(8)	2.027(4)	Fe(1)–C(9)	2.039(4)
Fe(1)–C(10)	2.042(4)	Fe(2)–C(21)	2.042(4)	Fe(2)–C(22)	2.051(4)
Fe(2)–C(23)	2.042(4)	Fe(2)–C(24)	2.040(4)	Fe(2)–C(25)	2.030(4)
Fe(2)–C(26)	2.053(4)	Fe(2)–C(27)	2.053(4)	Fe(2)–C(28)	2.045(4)
Fe(2)–C(29)	2.034(4)	Fe(2)–C(30)	2.041(4)	C(1)–C(11)	1.476(5)
C(6)–C(26)	1.463(5)	C(11)–O(12)	1.210(5)	C(11)–C(13)	1.503(5)
C(21)–C(31)	1.473(5)	C(31)–N(32)	1.271(5)	C(31)–C(43)	1.506(5)
C(31)–C(43)	1.506(5)	N(32)–C(33)	1.441(5)	ringI–Fe(1)	1.642(2)
ringII–Fe(1)	1.643(2)	ringIII–Fe(2)	1.654(2)	ringIV–Fe(2)	1.648(2)
Angles					
C(1)–Fe(1)–C(10)	107.6(2)	C(2)–Fe(1)–C(9)	109.4(2)	C(3)–Fe(1)–C(8)	108.6(2)
C(4)–Fe(1)–C(7)	106.5(2)	C(5)–Fe(1)–C(6)	105.6(2)	C(21)–Fe(2)–C(28)	113.4(2)
C(22)–Fe(2)–C(29)	111.6(2)	C(23)–Fe(2)–C(30)	109.3(2)	C(24)–Fe(2)–C(26)	109.5(2)
C(25)–Fe(2)–C(27)	111.7(2)				

TABLE 5. Atomic parameters  $x$ ,  $y$ ,  $z$  and  $B_{\text{iso}}$  for 2; e.s.d.s. refer to the last digit printed

	$x$	$y$	$z$	$B_{\text{eq}}$
Fe1	0.46075(5)	0.76949(5)	0.17317(5)	2.73(3)
Fe2	0.06356(5)	1.06165(6)	0.29068(5)	2.83(3)
C1	0.6087(3)	0.8676(3)	0.2186(3)	2.89(20)
C2	0.6450(4)	0.7301(4)	0.1656(4)	3.53(22)
C3	0.6146(4)	0.6759(4)	0.2446(4)	4.10(25)
C4	0.5584(4)	0.7767(4)	0.3462(4)	4.0(3)
C5	0.5541(4)	0.8957(4)	0.3315(4)	3.42(22)
C6	0.2835(3)	0.8560(4)	0.1653(3)	2.84(21)
C7	0.2891(4)	0.7319(4)	0.1716(4)	3.43(23)
C8	0.3426(4)	0.6367(4)	0.0648(4)	4.13(24)
C9	0.3686(4)	0.7006(4)	-0.0090(4)	3.88(23)
C10	0.3327(4)	0.8359(4)	0.0527(3)	3.03(21)
C11	0.6134(3)	0.9583(4)	0.1566(4)	2.95(20)
O12	0.6544(3)	0.9207(3)	0.0556(3)	4.08(16)
C13	0.5640(4)	1.0988(4)	0.2233(4)	4.2(3)
C21	-0.1154(3)	1.1369(3)	0.3124(3)	2.65(20)
C22	-0.0874(4)	1.0192(4)	0.3365(4)	3.04(21)
C23	-0.0493(4)	0.9181(4)	0.2240(4)	3.44(22)
C24	-0.0538(4)	0.9711(4)	0.1305(4)	3.43(22)
C25	-0.0933(4)	1.1052(4)	0.1841(4)	3.09(22)
C26	0.2414(3)	0.9822(4)	0.2612(4)	2.97(22)
C27	0.2153(4)	1.1044(4)	0.2460(4)	3.7(3)
C28	0.1817(4)	1.2010(4)	0.3635(4)	4.8(3)
C29	0.1857(4)	1.1402(4)	0.4500(4)	4.9(3)
C30	0.2227(4)	1.0057(4)	0.3878(4)	3.74(24)
C31	-0.1591(4)	1.2660(4)	0.4048(4)	3.06(21)
N32	-0.1937(3)	1.2701(3)	0.5058(3)	4.07(20)
C33	-0.2401(4)	1.3930(4)	0.5988(4)	3.44(23)
C34	-0.1562(4)	1.4598(3)	0.7037(4)	3.08(21)
C35	-0.0281(4)	1.4184(4)	0.7172(4)	3.74(23)
C36	0.0482(4)	1.4888(4)	0.8217(4)	4.7(3)
C37	0.0006(4)	1.6030(4)	0.9155(4)	4.7(3)
C38	-0.1210(4)	1.6452(4)	0.9067(4)	3.83(24)
C39	-0.2036(4)	1.5757(4)	0.8020(4)	3.12(22)
C40	-0.3315(4)	1.6186(4)	0.7923(4)	3.56(23)
C41	-0.4102(4)	1.5485(4)	0.6895(4)	4.22(25)
C42	-0.3620(4)	1.4342(4)	0.5918(4)	3.8(3)
C43	-0.1625(5)	1.3821(4)	0.3702(4)	4.9(3)

The main absorption bands from CO and CN stretching vibrations in compounds 1 and 2 and their oxidized salts are shown in Table 6, and reveal the wave number for the CO and CN stretches in the unoxidized compounds are shifted to lower wave number upon oxidation. The CO band at  $1646\text{ cm}^{-1}$  for 1 is shifted to lower wave number to  $1634\text{ cm}^{-1}$ , on formation of the salt with  $\text{I}_5^-$  (1a). The  $\text{FeCl}_4^-$  (1b) and  $\text{CuI}_2^-$  (1c) salts of 1 have these CO absorption bands at  $1646\text{ cm}^{-1}$  and  $1628\text{ cm}^{-1}$ , respectively. For 1b, the absorption is at  $1646\text{ cm}^{-1}$ , the same position as that for 1, implying that one acetyl substituent has remained in an unchanged chemical environment upon oxidation with  $\text{FeCl}_3$ . However, the position of the CO stretching for 1c,  $1628\text{ cm}^{-1}$ , is shifted to lower wave number relative to that for unoxidized 1; this shift could be attributed to oxidation of acetyl-substituted

ferrocenyl site and strong interaction between carbonyl group of the acetyl-substituent with the anion  $\text{CuI}_2^-$  which leads to decrease in the CO bond order.

The observed cyclovoltammogram of compound 1 reveals two successive reversible one electron oxidations ( $E_{1/2}(1) = 0.73$  and  $E_{1/2}(2) = 1.07$  V), which yield the corresponding mono-cation  $\text{CH}_3\text{CO-Fc-Fc}^+-\text{COCH}_3$  and dication  $\text{CH}_3\text{CO-Fc}^+-\text{Fc}^+-\text{COCH}_3$  respectively. The difference between  $E_{1/2}(1)$  and  $E_{1/2}(2)$  of 0.34 V, which should provide a good indication for the classification of the type of mixed-valence biferrocene derivatives [6]. However, in the case of asymmetric 1',1'''-substituted biferrocene 2, three half-wave potentials are observed. The potentials of the first  $E_{1/2}(1)$ , 0.66, and the second  $E_{1/2}$ , 0.97 V, are lower than those for 1 but the third  $E_{1/2}(3)$ , 1.16 V, is higher than  $E_{1/2}(2)$  for 1. This observation implies that one of three potential waves, presumably the lower value of 0.66 V, is to be attributed to oxidation of the naphthylimino moiety; *i.e.* to  $-\text{C}(\text{CH}_3)=\text{N}^+-\text{np}$  or  $-\text{C}(\text{CH}_3)=\text{N}-\text{np}^+$ .

The  $^{57}\text{Fe}$  Mössbauer spectral parameters at various temperatures of the compounds are listed in Table 3, and representative spectra are shown in Figs. 4–6. It is clear from Fig. 4 that the spectra obtained at 190 and

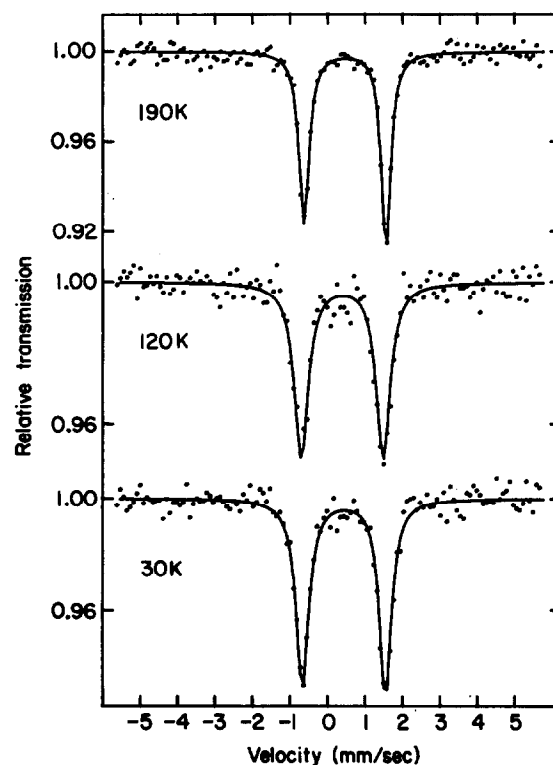


Fig. 4.  $^{57}\text{Fe}$  Mössbauer spectra of  $(\text{CH}_3\text{CO-Fc-Fc-C}(\text{CH}_3)=\text{N})_2^+ \text{I}_3^-$  (2a).

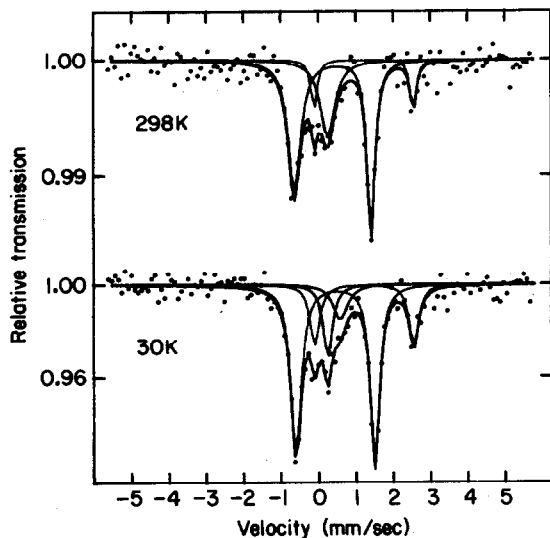


Fig. 5.  $^{57}\text{Fe}$  Mössbauer spectra of  $(\text{CH}_3\text{CO-Fc-Fc-COCH}_3)^+ \text{FeCl}_4^-$  (**1b**).

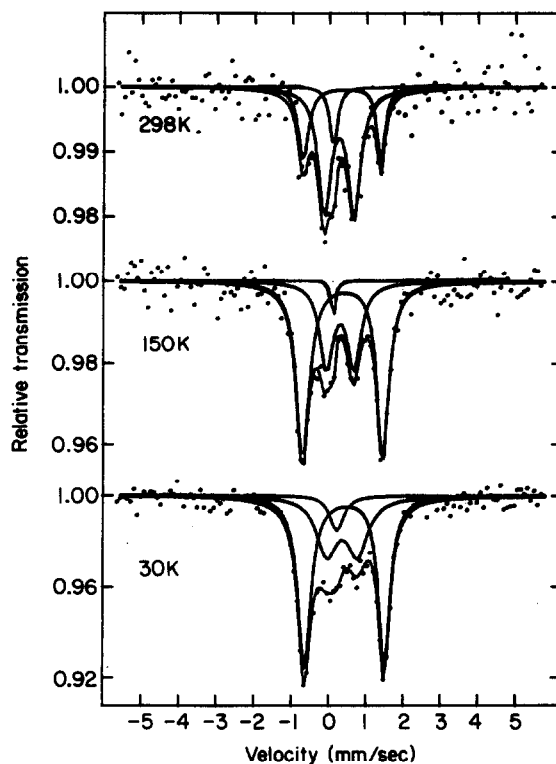


Fig. 6.  $^{57}\text{Fe}$  Mössbauer spectra of  $(\text{CH}_3\text{CO-Fc-Fc-C}(\text{CH}_3)=\text{N-np})^+ \text{FeCl}_4^-$  (**2b**).

30 K for **2a** ( $\text{I}_3^-$  salt of **2**) show a single doublet with Q.S. values of 2.18 and 2.20  $\text{mm s}^{-1}$ , with I.S. = 0.52 and 0.53  $\text{mm s}^{-1}$ , respectively. These values are close to those for the corresponding unoxidized **2** (as shown in Table 1). There is no oxidized ferrocenium ( $\text{Fc}^+$ ) form observed in the spectra, supporting the conclusions from the infrared and cyclic voltammetric studies.

The Mössbauer spectra at 298 and 30 K for  $\text{FeCl}_4^-$  salts of **1b** and **2b** are shown in Figs. 5 and 6. As can be seen from Fig. 5 the fitted spectra at 298 K for **1b** show two quadrupole doublets with outer large values of Q.S. (2.57  $\text{mm s}^{-1}$ ) and I.S. (1.30  $\text{mm s}^{-1}$ ), and inner medium values of Q.S. (2.06  $\text{mm s}^{-1}$ ) and I.S. (0.47  $\text{mm s}^{-1}$ ), and one singlet with an unresolvable Q.S.

(I.S. = 0.31  $\text{mm s}^{-1}$ ), which are ascribed to  $\text{FeCl}_2 \cdot 4\text{H}_2\text{O}$  [16], ferrocene-like  $\text{Fe}^{\text{II}}$  in the diacetylferrocenium cation, and high-spin  $\text{Fe}^{\text{III}}$  species in  $\text{FeCl}_4^-$  anion, respectively. However, at 30 K, an additional singlet with an unresolvable Q.S., with I.S. = 0.53  $\text{mm s}^{-1}$ , characteristics of ferricinium-like  $\text{Fe}^{\text{III}}$  appeared. In the spectra of **2b** at 298 and 30 K (see Fig. 6) three

TABLE 6. IR and Mössbauer data for the substituted biferrocenes and their salts

	IR ( $\text{cm}^{-1}$ )			Mössbauer parameter ( $\text{mm s}^{-1}$ )				Assignment
	C-H bonding ( $\pi\text{-C}_5\text{H}_5$ )	$\nu(\text{C}=\text{O})$	$\nu(\text{C}=\text{N})$	Q.S. 298 K	30 K	I.S. 298 K	30 K	
<b>1</b>	814	1646	—	2.19	2.21	0.48	0.53	Fc
<b>1a</b>	823	1634	—	2.08	2.13	0.45	0.53	Fc
	854	—	—	0	0	0.42	0.49	$\text{Fc}^+$
<b>1b</b>	829	1628	—	2.20	2.21	0.46	0.52	Fc
	845	—	—	0	0	0.23	0.34	$\text{Fc}^+$
<b>1c</b>	820	1646	—	2.57	2.68	1.30	1.32	$\text{FeCl}_2 \cdot 4\text{H}_2\text{O}$
	835	—	—	2.06	2.11	0.47	0.52	Fc
	—	—	—	0	0	0.31	0.34	$\text{FeCl}_4^-$
<b>2</b>	—	—	—	—	0	—	0.53	$\text{Fc}^+$
<b>2a</b>	829	1645	1612	2.19	2.21	0.47	0.54	Fc
<b>2a</b>	829	1628	1574	2.18 <sup>a</sup>	2.20	0.49 <sup>a</sup>	0.52	Fc
<b>2b</b>	831	1629	1577	2.12	2.19	0.45	0.55	Fc
	850	—	—	0.80	0.82	0.37	0.48	$\text{Fc}^+$
	—	—	—	0	0	0.28	0.35	$\text{FeCl}_4^-$

<sup>a</sup> Observed at 190 K.

components of iron species characteristic of ferrocene-like  $\text{Fe}^{\text{II}}$ , ferrocenium-like  $\text{Fe}^{\text{III}}$  and tetrachloroferrate  $\text{Fe}^{\text{III}}$  are observed, but there is no  $\text{FeCl}_2 \cdot 4\text{H}_2\text{O}$ . In addition, the proportion of ferrocenium-like  $\text{Fe}^{\text{III}}$  decreased with decreasing temperature. This implies that at low temperature (30 K) the salt undergoes a retro charge-transfer conversion from anion to a ferrocenium-like species or temperature-dependent intramolecular charge-transfer between the naphthylimino and ferrocenium-like species one of which is probably  $\text{CH}_3\text{CO}-\text{Fc}-\text{Fc}^+-\text{C}(\text{CH}_3)=\text{N}-\text{np} \leftrightarrow \text{CH}_3\text{CO}-\text{Fc}-\text{Fc}-\text{C}(\text{CH}_3)=\text{N}^+-\text{np}$  [15].

#### Acknowledgment

Support from the National Science Council of Taiwan (NSC80-208M032-08) is gratefully acknowledged.

#### References

- 1 D.B. Brown (ed.), *Mixed-Valence Compound. Theory and Applications in Chemistry, Physics, Geology and Biology*, D. Reidel, Boston, MA, 1979.
- 2 S. Nakashima, Y. Masuda, I. Motoyama and H. Sano, *Bull. Chem. Soc. Jpn.*, **60** (1987) 1673.
- 3 M. Kai, M. Katada and H. Sano, *Chem. Lett.*, (1989) 1473.
- 4 T.Y. Dong and T.L. Hsu, *J. Organomet. Chem.*, **367** (1989) 313.
- 5 T.Y. Dong and C.C. Schei, T.L. Hsu, S.L. Lee and S.J. Li, *Inorg. Chem.*, **30** (1991) 2457.
- 6 K. Suto, M. Katada, I. Motoyama and H. Sano, *Chem. Lett.*, (1985) 433.
- 7 M. Kai, M. Katada and H. Sano, *Chem. Lett.*, (1988) 1523.
- 8 D.O. Cowan, C. Levanda, J. Park and F. Kaufman, *Acc. Chem. Res.*, **6** (1973) 1.
- 9 M.D. Rausch, *J. Org. Chem.*, **29** (1964) 1257.
- 10 W.H., Jr. Morrison and D.N. Hendrickson, *Inorg. Chem.*, **14** (1975) 2331.
- 11 Z. Kaluski and A.I. Gusev, *Bull. Acad. Pol. Sci., Sci. Chim.*, **22** (1974) 739.
- 12 T.Y. Dong, D.N. Hendrickson, K. Iwai, M.J. Cohn, S.J. Geib, A.L. Rheingold, H. Sano I. Motoyama and S. Nakashima, *J. Am. Chem. Soc.*, **107** (1985) 7996.
- 13 P. Seiler and J.D. Dunitz, *Acta Crystallogr., Sect., B*, **35** (1979) 1068.
- 14 J.A. Kramer and D.N. Hendrickson, *Inorg. Chem.*, **19** (1980) 3330.
- 15 C.J. Lee and H.H. Wei, *J. Chin. Chem. Soc. (Taipei)*, **38** (1991) 143.